Applications and Applied Mathematics: An International Journal (AAM)

Volume 13 | Issue 2 | Article 18

12-2018

Thermoelastic stress analysis of a functionally graded transversely isotropic hollow cylinder in elliptical coordinates

Tara Dhakate
M.G. College, Armori,

Vinod Varghese
Smt. Sushilabai Rajkamalji Bharti Science College

Lalsingh Khalsa
M.G. College, Armori,

Available at
http://pvamu.edu/aam
Appl. Appl. Math.
ISSN: 1932-9466
Vol. 13, Issue 2 (December 2018), pp. 892–914

Applications and Applied
Mathematics:
An International Journal
(AAM)

Thermoelastic stress analysis of a functionally graded transversely isotropic hollow cylinder in elliptical coordinates

[1]Tara Dhakate, [2]Vinod Varghese, and [1]Lalsingh Khalsa

[1]Department of Mathematics
M.G. College
Armori, Gadchiroli, India
tarasadawarti@gmail

[2]Department of Mathematics
Smt. Sushilabai Rajkamalji Bharti Science College
Arni, Yavatmal, India
vino7997@gmail.com

Received: September 22, 2017; Accepted: September 6, 2018

Abstract

This paper is concerned with the axisymmetric thermoelastic problem to investigate the influence of nonlinear heat conduction equation, displacement functions and thermal stresses of a functionally graded transversely isotropic hollow cylinder that is presented in the elliptical coordinate system. The method of integral transform technique is used to produce an exact solution of the heat conduction equation in which sources are generated according to a linear function of the temperature. An explicit exact solution of the governing thermoelastic equation is proposed when material properties are power-law functions with the exponential form of the radial coordinate. Numerical calculations are also carried out for Material I with the nearly isotropic feature, along with Material II as an anisotropic material and illustrated graphically. The validity of the solution is demonstrated by comparing with the previous results.

Keywords: Elliptical coordinates; hollow cylinder; thermoelastic; integral transform; functionally graded material; transversely isotropic

MSC 2010 No.: 74E05, 34A25, 74A10, 33C05, 74G50

1. Introduction

The concept of functionally graded materials (FGMs) has been proposed at the beginning of the 90's by Japanese researchers. FGMs are characterised by continuous or step-wise varying compositions within the material. The mathematical modeling of FGMs is currently an active research area because of its increasing application in industrial engineering. Since the mathematical problems arising are complicated, a significant part of the work on FGMs has been carried out numerically, e.g. using finite element method (FEM), perturbation method and so on.

It has become necessary to develop other approaches for such a problem, particularly boundary value problems, which provide an invaluable check on the accuracy of numerical or approximate schemes and allow for widely relevant parametric studies. So, it is meaningful to examine the thermoelastic behaviour with defined boundary conditions. Thus, uniformly loaded homogeneous and isotropic plate has attracted the focus of the researchers over the past several years owing to its application on various machines and structures.

In past some authors have undertaken the work on uniformly loaded functionally graded (FG) structures, which can be summarised as given below. [Obata and Noda (1994)] used Laplace transformation and perturbation method to obtain one-dimensional steady thermal stress response in a hollow circular cylinder and a hollow sphere based on the perturbation method. [Horgan and Chan (1999)] analysed the classic problem of stress distribution in an inhomogeneous isotropic rotating solid disc and pressurised hollow cylinder. [Lutz and Zimmerman (1999)] have presented a solution to the issue of the uniform heating of an FG cylinder with simple forms for the variation of the moduli with radius using the method of Frobenius series. [Chen et al. (2002); Chen et al. (2001)] in his axisymmetric thermoelastic problem of a uniformly heated FG isotropic hollow cylinder and cylindrical shell of finite length investigated thermal stress effect. [Wang et al. (2004)] obtained the analytical solutions of stresses in FG circular hollow cylinder with finite length using Sine transform, which was expressed in a triangle and power series. [Varghese and Khobragade (2008); Varghese and Khobragade (2008); Kamdi et al. (2008)] studied the displacement and stress functions of an FGM subjected to a uniform temperature field with thermo-mechanical boundary conditions taking various material profiles.

Recently, [Abrinia et al. (2008)] proposed a new analytical solution for computing the radial and circumferential stresses in an FGM thick cylindrical vessel under the influence of internal pressure and arbitrary steady state temperature field, by using the variation of parameters method (Lagrange). Therefore, a number of theoretical studies on different objects have been reported so far. However, to simplify the analysis, almost all research was carried out with uniform temperature distribution throughout the surfaces. However, only a few studies concerned with heat conduction problems in elliptical objects were observed.

Very recently, [Hsieh et al. (2006)] investigated the inverse issue of an FGM elliptical plate with large deflection based on the classical nonlinear von Karman plate theory and solved the nonclassical problem using a perturbation technique. [Kumar et al. (2009)] performed the parametric studies on the prediction of vibro-acoustic response from an elliptic disc made up of FGM by using the finite element method. [Cheng et al. (2000)] obtained a closed form solution for thermo-mechanical deformations of an isotropic linear thermoelastic FG elliptic plate rigidly clamped at the edges in which the effective material properties at a point were computed by the Mori Tanaka scheme. Recently, [Asemi et al. (2013)] studied the static and dynamic behaviours of FGMs elliptical plates based on the principle of minimum potential energy and Rayleigh-Ritz method. [El Dhaba et al. (2003)] used boundary integral method to solve the problem of the plane, uncoupled linear thermoelasticity with heat sources for an infinite cylinder with the elliptical cross-section, subjected to a uniform pressure having thermal radiation condition at its boundary. [Hasheminejad et al. (2011)] obtained an exact solution for the dynamic response of an elastic elliptical membrane by employing eigenfunction expansion in terms of transcendental and modified Mathieu functions. [Khorshidvand et al. (2010); Khorshidvand and Jabbari (2012); Khorshidvand and Jabbari (2012)] presented a new solution for one-dimensional steady-state mechanical and thermal stresses in an FG rotating thick hollow cylinder and disk farmed in elliptical coordinate system assuming the temperature distribution to be a function of radius along the thickness, with general thermal and mechanical boundary conditions on the surface of the cylinder. Very recently, [Bhad et al. (2016); Bhad et al. (2017); Bhad et al. (2017); Bhad et al. (2017)] obtained few solutions for the governing equation considering internal heat generation within the homogeneous elliptical objects in elliptical coordinates applying few extended integral transforms.

In all the above cited literature, the authors have not taken into consideration any thermoelastic problem for hollow cylinder expressed in elliptical coordinates [i.e. projecting the two-dimensional elliptic coordinate system in the perpendicular z-direction] with boundary conditions of radiation type, in which heat sources are generated according to the linear function of the temperatures, which satisfies the time-dependent heat conduction equation. It has been noticed that heat production in solids have led to various technical problems in mechanical applications in which heat produced is rapidly sought to be transferred or dissipated. For instance, gas turbines blades, walls of the internal combustion engine (ICE), the outer surface of a space vehicle, etc. all depend for their durability on rapid heat transfer from their surfaces. Things get further complicated when internal heat generation persists on the object under consideration. This further becomes unpredictable when sectional heat supply is impacted on the body. Both analytical and numerical techniques have proved to be the best methodology to solve such problems. Nonetheless, numerical solutions are preferred and prevalent in practice, due to either the non-availability or mathematical complexity of the corresponding exact solutions. Rather, limited utilization of analytical solutions should not diminish their merit over numerical ones; since exact solutions, if available, provide an insight into the governing physics of the problem, that is often missing in any numerical solution. Moreover, analysing closed-form solutions to obtain optimal design options for any particular application of interest is relatively simpler. However, to the best of authors knowledge, no work has been published till date to determine the temperature distribution and its associated stresses of a functionally graded hollow cylinder considering internal heat supply with boundary conditions of radiation type on the outside and inside surfaces, with independent radiation constants. Owing to the lack of research in FG cylindrical objects in the elliptical coordinate system, the authors have been motivated to conduct this study.

This paper dealt with the theoretical treatments of a hollow cylinder occupying the space $D =$

$(\xi, \ell) \in R^2 : a \leq \xi \leq b, z \in (0,\, \ell)$ having radiation type boundary conditions on both surfaces impacted by arbitrary initial temperature. The solution to the heat conduction equation is obtained using a new integral transformation involving ordinary and modified Mathieu functions of first and second kind of order n. Inversion formula has been established, and some properties are mentioned. The general solution of displacement formulation is obtained by the introduction of appropriate transformation, and the analyses are carried out by taking parameters of the exponential profile. The theoretical calculation has been considered using the dimensional parameter, whereas, graphical calculations are made using the dimensionless parameter. The success of this research mainly lies on the new mathematical procedures which present a rather simpler approach for optimization of the design in terms of material usage and performance in engineering problem, particularly in determining thermoelastic behaviour. During the designing phase, both the elliptical and cylindrical curved structures are taken on a common coordinate system, i.e. either elliptic, cylindrical or elliptical-cylindrical coordinate system. For example, in a nuclear reactor, particularly intercoolers, pressure vessels or furnaces, a combination of different curved profiles are needed. Most of the investigation on hollow elliptical patterns mentioned above in the elliptical-cylindrical coordinate system has already been discussed. In this manuscript, we intend to study the thermoelastic behaviour considering hollow circular objects in the elliptical-cylindrical coordinate system as a novel approach.

2. Notation and governing equations

Consider a transversely isotropic elastic body of finite length ℓ occupying the space *D* in the elliptical coordinate system. The cylinder is bounded by the region $a \leq \xi \leq b$, where a and b denote the inner and outer radii respectively, whereas $0 \leq z \leq \ell$ and η is constant [i.e. geometry parameters are denoted as $\xi \in [a,\, b]$ and $z \in (0,\, \ell)$]. Here we assume that when a semi-focal length parameter '*c*' approaches zero value, the elliptical surface goes to a cylindrical surface. Thus, it will bring about $\sinh \xi = \cosh \xi$, and in this particular case, the equation of hollow cylinder can be stated as $x^2 + y^2 = c^2 \cosh^2 \xi$ [Khorshidvand et al. (2010); Khorshidvand and Jabbari (2012); Khorshidvand and Jabbari (2012)] in which $c \cosh \xi$ represents the radius of the cylinder. The curves $\eta =$ constant constitute a family of confocal hyperbolas while the curves $\xi =$constant pose a family of confocal ellipses (refer to Figure 1). Both sets of curves intersect each other orthogonally at every point in space. The displacement components are indicated by $(u_\xi,\ 0,\ u_z)$ and stress components by $\sigma_{\xi\xi},\ \sigma_{\eta\eta}$ etc. In this problem, we assume that the material parameters $c_{ij}\,(i, j = 1,\, 2, 3)$ and the thermal expansion coefficient $\alpha_i\,(i = 1,\, 3)$ are functions of ξ but not of η and z.

2.1. Basic equations

The basic equations corresponding to the transversely isotropic functionally graded materials can be summarised as follows [Khorshidvand et al. (2010)]:

(1) Strain-displacement relationships:

$$\varepsilon_{\xi\xi} = \frac{1}{c\,\cosh\,\xi}\frac{\partial u_\xi}{\partial \xi}, \varepsilon_{\eta\eta} = \frac{u_\xi}{c\,\cosh\,\xi}, \varepsilon_{zz} = \frac{\partial u_z}{\partial z}. \tag{1}$$

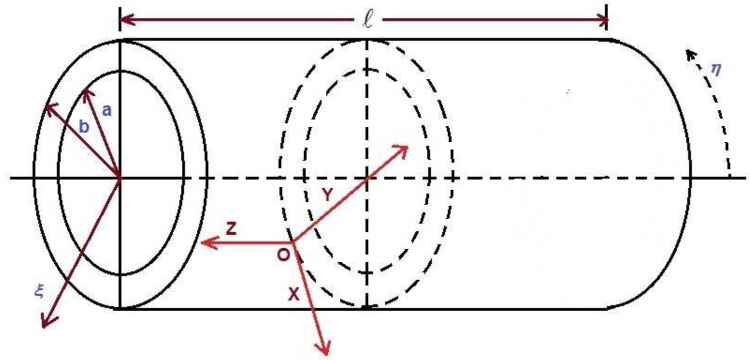

Figure 1. Cylinder configuration in elliptical coordinates

(2) Equilibrium equations for axisymmetric stresses in the presence of body force, reduced to the single equation:

$$\frac{1}{a\,\cosh\,\xi}\left\{\frac{\partial}{\partial\xi}\sigma_{\xi\xi}+(\sigma_{\xi\xi}-\sigma_{\eta\eta)}\right\}+\rho\,F_{\xi}=0, \tag{2}$$

with ρ as the mass density and F_{ξ} as the body force.

(3) Stress components in terms of infinitesimal strains and the temperature in a stress-free state are denoted as:

$$\left.\begin{aligned}\sigma_{\xi\xi}&=c_{11}\,\varepsilon_{\xi\xi}+c_{12}\,\varepsilon_{\eta\eta}+c_{13}\,\varepsilon_{zz}-\beta_1\,T(\xi,z,t),\\ \sigma_{\eta\eta}&=c_{12}\,\varepsilon_{\xi\xi}+c_{11}\,\varepsilon_{\eta\eta}+c_{13}\,\varepsilon_{zz}-\beta_1\,T(\xi,z,t),\\ \sigma_{zz}&=c_{13}\left[\varepsilon_{\xi\xi}+\varepsilon_{\eta\eta}\right]+c_{33}\,\varepsilon_{zz}-\beta_3\,T(\xi,z,t),\end{aligned}\right\} \tag{3}$$

in which we assume $\sigma_{\xi z}=\sigma_{\xi\eta}=\sigma_{\eta z}=0$.

The stress-temperature coefficient $\beta_i(i=1,\,3)$ is related to α_i and indicated as $\beta_1=(c_{11}+c_{12})\alpha_1+c_{13}\alpha_3,\ \beta_3=2c_{13}\alpha_1+c_{33}\alpha_3$ with body force as $F_{\xi}=0$, $T(\xi,z,t)$ is the temperature of the plate at a point (ξ,z) in time t, and c_{ij} is the elastic coefficient parameter.

Substituting the Equations (1) and (3) in Equation (2), the thermoelastic equilibrium equation of the hollow cylinder can be obtained as

$$\frac{1}{c\,\cosh\,\xi}\left\{c_{11}\frac{\partial^2u_{\xi}}{\partial\xi^2}+c_{11}'\frac{\partial u_{\xi}}{\partial\xi}+(c_{12}'-c_{11})\,u_{\xi}\right\}=[\beta_1T]'-c_{13}'\,\frac{\partial u_z}{\partial z}, \tag{4}$$

where the prime $(')$ denotes differentiation with respect to ξ.

2.2. Boundary conditions

For a complete solution as suggested by [Spencer et al. (1992)] to the thermoelastic problem, displacement field is to be determined such that for $T\neq\ 0$; zero traction is noticed on all surfaces of the hollow cylinder. Thus we assume the following:

(1) Zero traction conditions on the inner and outer curved surfaces

$$\sigma_{\xi\xi} = 0,\ \sigma_{\xi\eta} = 0,\ \sigma_{\xi z} = 0 \ \text{ at } \ \xi = a,\ b. \tag{5}$$

(2) Zero normal force on $z = 0,\ \ell$:

$$2\pi \int_a^b \sigma_{zz}\, \xi\, d\xi \ = \ 0. \tag{6}$$

(3) Boundary conditions of the finite length hollow cylinder be simply supported at the two longitudinal edges, i.e.,

$$\sigma_{zz} = 0,\ \ \sigma_{\eta z} = \ 0,\ \ \sigma_{\xi z} = 0 \ \text{ at } \ z = 0,\ \ell. \tag{7}$$

As the problem is concerned with the radial direction only, we have not considered zero resultant force and bending moment at the edges $\eta = 0,\ \eta_0$. It has been learned from the previous literature that the solution may leave un-equilibrated bending moment and a shear force on the ends of the finite length functionally graded hollow cylinder. To neutralise this moment and force, it requires an additional solution that involves stress that depends on the angle η as well as variable ξ.

3. Heat transfer formulation

The governing equation of heat conduction with internal heat source in elliptical coordinates as

$$h^2 \frac{\partial}{\partial \xi}\left(\lambda(\xi)\frac{\partial T}{\partial \xi}\right) + \frac{\partial}{\partial z}\left(\lambda(\xi)\frac{\partial T}{\partial z}\right) + \Theta\,(\xi,\ z,\ t,\ T) = c_v(\xi)\,\rho\,\frac{\partial T}{\partial t}, \tag{8}$$

subjected to the following initial and boundary conditions

$$T(\xi,\ z, 0) = T_0, \tag{9}$$

$$\frac{\partial}{\partial \xi} T(a,\ z,\ t) + k_1\, T(a,\ z,\ t) = 0, \tag{10}$$

$$\frac{\partial}{\partial \xi} T(b,\ z,\ t) + k_2\, T(b,\ z,\ t) = 0, \tag{11}$$

$$T(\xi, 0, t) = 0, \tag{12}$$

$$T(\xi, \ell, t) = 0, \tag{13}$$

in which $\lambda(\xi)$ is the coefficient of thermal conductivity along the respective directions, $c_v(\xi)$ is the heat capacity, $\Theta(\xi, z, t,\ T)$ is the source function, $k_i\,(i = 1, 2)$ are the given surface coefficients linearly related to the corresponding heat transfer coefficients at the internal and external radial surfaces $\xi = a$ and $\xi = b$, T_0 represents the initial temperature at $t = 0$, and the metric coefficient is given as

$$h^2 = 2/(c^2 \cosh 2\xi). \tag{14}$$

4. Reformulation of the problem

In a related theoretical study done by [Horgan and Chan (1999)] and [Chen et al. (2002); Chen et al. (2001)], the variation in thermo-mechanical properties was described by the nonlinear function as a simple power law model. As pointed out by [Eraslan and Akis (2005)], their model is not as flexible as the general parabolic model. Here, we have considered the functionally graded material with non-constant elastic parameters that vary exponentially along the radius. With this general exponential model, a wide range of nonlinear and continuous profiles can be obtained to describe the reasonable variation in the thermoelastic properties giving the minimum stress level. For theoretical treatments, we consider the elastic coefficient parameter c_{ij}, thermal expansion coefficient α_i, and the thermal conductivity λ_i, and heat capacity coefficient c_v as

$$c_{ij} = c_{ij}^0\,(\gamma\, e^{k\xi}),\;\; \alpha_i = \alpha_i^0\,(\gamma\, e^{k\xi}),\; \lambda_i = \lambda^0\,(\gamma\, e^{k\xi}),\;\; c_v = c_v^0(\gamma\, e^{k\xi}),\;\; \rho = \rho^0, \tag{15}$$

in which c_{ij}^0, α_i^0, λ^0, c_v^0 and ρ^0 are arbitrary constants having the same dimension as c_{ij}, α_i, λ, c_v and ρ respectively; γ and k are the physical parameters whose combination forms a broad range of nonlinear and continuous profiles to describe the reasonable variation of material constants and thermal expansion coefficients.

5. Heat conduction reformulation

Using equation (15) in equation (8), we obtain

$$h^2\left(\frac{\partial^2 T}{\partial \xi^2} + k\,\frac{\partial T}{\partial \xi}\right) + \frac{\partial^2 T}{\partial z^2} + \frac{\Theta\;(\xi,\; z,\; t,\; T)}{\gamma\, e^{k\xi}\,\lambda^0} = \frac{c_v^0\,\rho^0}{\lambda^0}\;\frac{\partial T}{\partial t}. \tag{16}$$

Now, we assume that $\Theta\;(\xi,\; z,\; t,\; T)$ is a known function of position, time and temperature, which can be taken in a manner [Sneddon (1995)] given below

$$\Theta\,(\xi,\, z,\, t,\, T) \;=\; \Phi\,(\xi,\, z,\, t) \;+\; \psi\,(t)\,\theta\,(\xi,\, z,\, t), \tag{17}$$

and

$$\left.\begin{aligned} \theta\,(\xi,\, z,\, t) \;&=\; T\,(\xi,\, z,\; t)\; e^{-\int_0^t \psi\,(\tau)\,d\tau},\\ \chi\,(\xi,\, z,\, t) \;&=\; \Phi\,(\xi,\, z,\, t)\, e^{-\int_0^t \psi\,(\tau)\,d\tau}, \end{aligned}\right\} \tag{18}$$

in which $\theta(\xi,\, z,\, t)$ is the temperature of the plate at a point (ξ, z) in time t, $\chi(\xi, z, t)$ is the energy generation, $\Phi\,(\xi,\, z,\, t)$ is a function of coordinates and the time, but $\psi\,(t)$ is a function of the time only.

Substituting equation (17) and (18) in the heat conduction equation (16), we assume the equivalent form as

$$h^2\left(\frac{\partial^2 \theta}{\partial \xi^2} + k\,\frac{\partial \theta}{\partial \xi}\right) + \frac{\partial^2 \theta}{\partial z^2} + \frac{Q_i\,\delta(z-\ell_0)\,f(t)}{\lambda^0} = \frac{1}{\kappa}\;\frac{\partial \theta}{\partial t}, \tag{19}$$

subjected to the following initial and boundary conditions

$$\theta(\xi,\ z, 0) = \theta_0, \tag{20}$$

$$\frac{\partial}{\partial \xi}\theta(a, z,\ t) + k_1\, \theta(a, z, t) = 0, \tag{21}$$

$$\frac{\partial}{\partial \xi}\theta(b, z,\ t) + k_2\, \theta(b, z, t) = 0, \tag{22}$$

$$\theta(\xi, 0, t) = 0, \tag{23}$$

$$\theta(\xi, \ell, t) = 0, \tag{24}$$

where $f(t)$ as a function of time *t,* and thermal diffusivity is taken as $\kappa = \lambda^0/\rho^0 c_v^0$. For the sake of brevity, we assume that there are physical situations wherein the rate of internal heat energy per unit volume is influenced by material properties that vary exponentially along the radius [that is, at position $(\xi,\ z\,)$] and with time *t*, which leads to

$$\chi\,(\,\xi,\ z\,,\, t) = \ Q_i\, \gamma\, e^{(k/2)\xi} \delta(z - \ell_0)\, f(t), 0 < \ell_0 < \ell,$$

wherein the initial temperature is taken as θ_0 and heat flux as Q_i.

5.1. Displacement equation reformulation

Using equation (15) in equation (4), we obtain a standard form of differential equation as

$$\frac{1}{c\cosh\xi}\left\{\frac{\partial^2 u_\xi}{\partial \xi^2} + k\frac{\partial u_\xi}{\partial \xi} - \left[1 - k(c_{12}^0/c_{11}^0)\right] u_\xi\right\} = -k(c_{13}^0/c_{11}^0)\frac{\partial u_z}{\partial z} + (\beta_1^0/c_{11}^0)\left[kT + \frac{\partial T}{\partial \xi}\right]. \tag{25}$$

Equation (25) is a differential equation, which can be solved by introducing a new function $u_\xi^*(\xi)$ and applying the transformations

$$u_\xi(\xi) = e^{-k\xi/2}\, u_\xi^*(\xi),\ \ u_\eta(\eta) = 0,\ \ u_z(z) = Gz, \tag{26}$$

with *G* as the unknown constant (that is, independent of variable ξ) and will be determined later. The term $u_\xi(\xi) = e^{-k\xi/2}\, u_\xi^*(\xi)$ represents a radial expansion or contraction in which, the inner and outer radii change, in general, whereas the angle remains constant and $u_z(z) = Gz$ is a uniform axial extension or contraction.

Substituting equation (26) into Equation (25), and rewriting the governing equation as

$$\frac{\partial^2 u_\xi^*}{\partial \xi^2} - \wp^2\, u_\xi^* = c\, e^{k\xi/2} \cosh\, \xi\, \{-kG\, (c_{13}^0/c_{11}^0) + (\beta_1^0/c_{11}^0)\, [kT + \frac{\partial T}{\partial \xi}]\}, \tag{27}$$

in which

$$\wp^2 = 1 + (k^2/2^2) - k(c_{12}^0/c_{11}^0).$$

The Equations (3), (8)-(13) and (27) constitute mathematical formulation of the problem under consideration.

6. Solution for the Problem

6.1. The solution for temperature profile

It is convenient to introduce a new dependent function $\vartheta(\xi, z, t)$ at the first instance in Equation (19) and boundary conditions (20)-(24)

$$\theta(\xi, z, t) = e^{-k\xi/2}\,\vartheta(\xi, z, t). \tag{28}$$

Substituting equation (28) in the heat conduction equation (19) and boundary conditions (20)-(24), we assume the equivalent form

$$h^2\left(\frac{\partial^2}{\partial \xi^2} - \frac{k^2}{2^2}\right)\vartheta(\xi,\, z, t) + \frac{\partial^2}{\partial z^2}\vartheta(\xi,\, z, t) + \frac{Q_i\,\delta(z-\ell_0)\,f(t)}{\lambda^0} = \frac{1}{\kappa}\,\frac{\partial}{\partial t}\vartheta(\xi,\, z, t), \tag{29}$$

subjected to the following initial and boundary conditions

$$\vartheta(\xi,\, z, 0) = \vartheta_0\, e^{k\xi/2}, \tag{30}$$

$$\frac{\partial}{\partial \xi}\,\vartheta(a, z,\; t) + \frac{k_1}{2}\,\vartheta(a, z, t) = 0, \tag{31}$$

$$\frac{\partial}{\partial \xi}\vartheta(b, z,\; t) + \frac{k_2}{2}\,\vartheta(b, z, t) = 0, \tag{32}$$

$$\vartheta(\xi, 0, t) = 0, \tag{33}$$

$$\vartheta(\xi, \ell, t) = 0. \tag{34}$$

Considering the finite Fourier-Sine transformation to the differential equation (29), and boundary conditions (33)-(34) into account, we get

$$h^2\left(\frac{\partial^2}{\partial \xi^2} - \frac{k^2}{2^2}\right)\bar{\vartheta}(\xi, n, t) - \frac{n^2\pi^2}{\ell^2}\bar{\vartheta}(\xi, n, t) + \frac{Q_i\bar{f}(t)}{\lambda^0}\sin\left(\frac{n\pi\ell_0}{\ell}\right) = \frac{1}{\kappa}\frac{\partial}{\partial t}\bar{\vartheta}(\xi, n, t), \tag{35}$$

in which *n* is the transformed parameter, $\bar{\vartheta}(\xi, n, t)$ and $\bar{f}(t)$ are the transformed function of $\vartheta(\xi, n, t)$ and $f(t)$ respectively.

After some algebraic calculation for Equation (35), it leads to considerable mathematical simplification as

$$\left\{\frac{\partial^2}{\partial \xi^2} - [\lambda^* + 2q^*\cosh 2\xi]\right\}\bar{\vartheta}(\xi, n, t) + \frac{Q_i\bar{f}(t)}{\lambda^0 h^2}\sin\left(\frac{n\pi\ell_0}{\ell}\right) = \frac{1}{\kappa h^2}\frac{\partial}{\partial t}\bar{\vartheta}(\xi, n, t), \tag{36}$$

moreover, the boundary as

$$\bar{\vartheta}(\xi,\, z, 0) = \vartheta_0\, e^{k\xi/2}, \tag{37}$$

$$\frac{\partial}{\partial \xi}\,\bar{\vartheta}(a,\, n,\, t) + \frac{k_1}{2}\,\bar{\vartheta}(a, n, t) = 0, \tag{38}$$

$$\frac{\partial}{\partial \xi}\bar{\vartheta}(b,\, n,\, t) + \frac{k_2}{2}\,\bar{\vartheta}(b,\, n,\, t) = 0, \tag{39}$$

in which

$$\lambda^* = k^2/4, 2q^* = c^2\left(n\pi/\ell\right)^2/2.$$

In order to solve hyperbolic type of differential Equation (36) using the theory on integral transformation, we firstly introduce a integral transform of order m over the variable ξ as

$$\left\{\begin{array}{c}\bar{f}(\ \ q_m)\\ \bar{f}(-q_m)\end{array}\right\} = \int_a^b \left\{\begin{array}{c}S_m(\alpha_1,\alpha_2,\xi,\ \ q_m)\\ S_m(\alpha_1,\alpha_2,\xi,-q_m)\end{array}\right\} \cosh(2\xi)\, f(\xi)\, d\xi. \tag{40}$$

Inversion theorem of (40) is

$$f(\xi) = \sum_{m=1}^{\infty} \left\{\begin{array}{c}\bar{f}(\ \ q_m)\\ \bar{f}(-q_m)\end{array}\right\} \left\{\begin{array}{c}S_m(\alpha_1,\alpha_2,\xi,\ \ q_m)\\ S_m(\alpha_1,\alpha_2,\xi,-q_m)\end{array}\right\} /N_m, \tag{41}$$

in which $\pm\, q_m$ is a root of a transcendental equation of

$$\frac{Ce_m(\alpha_1, a,\ \pm q_m)}{Ce_m(\alpha_2, b,\ \pm q_m)} - \frac{Fey_m(\alpha_1, a,\ \pm q_m)}{Fey_m(\alpha_2, b,\ \pm q_m)} = 0, \tag{42}$$

where the kernel is defined as

$$\begin{aligned} S_m(\alpha_1,\alpha_2,\xi,\ \pm q_m) = {} & Ce_m(\xi,\ \pm q_m)[Fey_m(\alpha_1, a,\ \pm q_m)\ + Fey_m(\alpha_2, b,\ \pm q_m)] \\ & - Fey_m(\xi,\ \pm q_m)\ [Ce_m(\alpha_1, a,\ \pm q_m)\ + Ce_m(\alpha_2, b,\ \pm q_m)]\,, \end{aligned} \tag{43}$$

in which

$$\left.\begin{array}{ll} Ce_m(\alpha_i, a, q) & = Ce_m(a,q) + \alpha_i\, Ce'_m(a,q), \\ Fey_m(\alpha_i, a, q) & = Fey_m(a,q) + \alpha_i\, Fe'y_m(a,q)\ , \end{array}\right\} (i = 1,\ 2)$$

and

$$N_m = \pi \int_a^b S_m^2(\alpha_1,\alpha_2,\xi,q_m)\, \cosh 2\xi\, d\xi,$$

whereas, $Ce_m(\xi, \pm q_m)$ and $Fey_m(\xi, \pm q_m)$ represents modified Mathieu function of first and second kind of order *m* respectively, which is denoted as $Ce_m(\xi,\ q) = \sum_{r=0}^{\infty} A_{2r}^{(m)} \cosh 2r\xi$, the recurrence [McLachlan (1947)]

$$Fey_m(\xi, q) = \frac{ce_{2n}(0,q)}{A_0^{(m)}} \sum_{r=0}^{\infty} A_{2r}^{(m)} Y_{2r}(2k' \sinh \xi) \begin{pmatrix} |\sinh \xi| > 1 \\ R(\xi) > 0 \end{pmatrix},$$

with *y* in *Fey* signifies the *Y*-Bessel function and $q = k'^2 = \lambda c^2/4$. The kernel of above transform is represented in the form of elliptical function, and it replaces the differential equation defined in (36) for the boundary conditions (37)-(39) of the third kind. The operational property is given as

$$\begin{aligned} \int_a^b \left(\frac{\partial^2 f}{\partial \xi^2}\right)\ S_m(\alpha_1,\alpha_2,\xi,q_m)\, d\xi = {} & \left(\alpha_2 \frac{\partial f}{\partial \xi} + f\right)\Big|_{\xi=b} S_m(\alpha_1,\alpha_2,b,q_m) \\ & + \left(\alpha_1 \frac{\partial f}{\partial \xi} + f\right)\Big|_{\xi=a} S_m(\alpha_1,\alpha_2,a,q_m) - 2q_m \bar{f}. \end{aligned} \tag{44}$$

On applying the proposed integral transform (40) to the differential Equation (36), and taking property (44) into account under the conditions (38) and (39), one obtains

$$\frac{\partial}{\partial t}\bar{\bar{\vartheta}}(q_m,\, n,t)+\kappa\,\lambda_m^2\,\bar{\bar{\vartheta}}(q_m,\, n,t)=\,\frac{Q_i\,\kappa}{\lambda^0}\,\bar{\bar{f}}(q_m,n,\,t), \tag{45}$$

in which

$$\lambda_m^2\,=\,4q_m/a^2,$$

subjected to the following initial conditions

$$\overline{\bar{\bar{\vartheta}}}(\xi,\,z,0)=\,\vartheta_0 G_0,$$

whereas,

$$G_0=\int_a^b S_m(\alpha_1,\alpha_{2,\xi,}q_m)\cosh 2\xi\;e^{k\xi/2}d\xi,$$

and

$$\bar{\bar{f}}(q_m,n,\,t)=\int_a^b\bar{\bar{f}}(\,t)\sin\left(\frac{n\pi\,\ell_0}{\ell}\right)\,S_m(k_1/2,k_2/2,\xi,-q_m)\cosh 2\xi\,d\xi,$$

in which $\bar{\bar{\vartheta}}(q_m,\,n,t)$ and $\bar{\bar{f}}(\,t)$ are the transformed functions of $\bar{\vartheta}(\xi,\,n,t)$ and $\bar{f}(\,t)$, respectively.

The general solution to the differential equation (45), taking the transformed initial condition (30) as $\vartheta(\xi,\,z,0)=\vartheta_0\,e^{k\xi/2}$ into account, leads to

$$\bar{\bar{\vartheta}}(q_m,\,n,t)=e^{-\kappa\,\lambda_m^2 t}\left(\vartheta_0\,G_0+\frac{Q_i\,\kappa}{\lambda^0}\int_0^t e^{\kappa\,\lambda_m^2\tau}\;\bar{\bar{f}}(q_m,n,\,\tau)\,d\tau\right). \tag{46}$$

Applying inversion theorems of the transform rules defined by Equation (41) on the equation (46), results into

$$\begin{aligned}\bar{\vartheta}(\xi,\,n,t)=&\textstyle\sum_{m=1}^{\infty}\,e^{-\kappa\,\lambda_m^2 t}\left(\vartheta_0 G_0+\frac{Q_i\,\kappa}{\lambda^0}\int_0^t e^{\kappa\,\lambda_m^2\tau}\;\bar{\bar{f}}(q_m,n,\,\tau)\,d\tau\right)\\&\times S_m(k_1/2,k_2/2,\xi,-q_m)/N_m.\end{aligned} \tag{47}$$

Further accomplishing inversion theorems of the finite Fourier-Sine transform on equation (47), the temperature is obtained as:

$$\begin{aligned}\vartheta(\xi,\,z,t)=&\textstyle\frac{2}{\ell}\sum_{n=0}^{\infty}\sum_{m=1}^{\infty}\left[e^{-\kappa\,\lambda_m^2 t}\left(\vartheta_0 G_0+\frac{Q_i\,\kappa}{\lambda^0}\int_0^t e^{\kappa\,\lambda_m^2\tau}\;\bar{\bar{f}}(q_m,n,\,\tau)\,d\tau\right)\right]\\&\times S_m(k_1/2,k_2/2,\xi,-q_m)\,\sin\left(\tfrac{n\pi\,z}{\ell}\right)/N_m.\end{aligned} \tag{48}$$

Taking into account Equation (28) and the first equation of Equation (18), the temperature distribution is finally represented by

$$\begin{aligned}T(\xi,z,t)=&\textstyle\left\{\frac{2}{\ell}e^{-k\xi/2}\sum_{n=0}^{\infty}\sum_{m=1}^{\infty}\left[e^{-\kappa\lambda_m^2 t}\left(\vartheta_0 G_0+\frac{Q_i\kappa}{\lambda^0}\int_0^t e^{\kappa\lambda_m^2\tau}\bar{\bar{f}}(q_m,n,\tau)d\tau\right)\right]\right.\\&\left.\times S_m(k_1/2,k_2/2,\xi,-q_m)\sin\left(\tfrac{n\pi z}{\ell}\right)/N_m\right\}\;e^{-\int_0^t\psi(\tau)d\tau}.\end{aligned} \tag{49}$$

The above function is given in Equation (49) represents the temperature at every instant and at all points of the hollow cylinder of finite height under conditions of radiation type on the surface.

6.2. The solution for displacement and thermal stresses

The general solution of non-homogeneous differential equation (27) can be expressed as a combination of complementary function and particular solution. It can be represented as

$$u_\xi^* = u_\xi^c + u_\xi^p, \tag{50}$$

then, the homogeneous solution can be expressed as

$$u_\xi^c = C_1\, e^{\xi\wp} + C_2\, e^{-\xi\wp}, \tag{51}$$

for the associated homogeneous equation

$$\frac{\partial^2 u_\xi^*}{\partial \xi^2} - \wp^2\, u_\xi^* = 0, \tag{52}$$

in which $C_i \quad (i = 1,\, 2)$ is an arbitrary integration constant to be determined.

The particular integral solution u_ξ^p of Equation (27) is determined by the method of variation of parameters. It is assumed to be of the form

$$u_\xi^p = \hat{U}_1\, e^{\xi\wp} + \hat{U}_2\, e^{-\xi\wp}, \tag{53}$$

where

$$W(\xi) = \det\begin{pmatrix} e^{\xi\wp} & e^{-\xi\wp} \\ \wp e^{\xi\wp} & -\wp e^{-\xi\wp} \end{pmatrix} = -2\wp, \tag{54}$$

$$\hat{U}_1 = \frac{1}{2\wp}\int_a^b e^{-\xi\wp} g(\xi)\, d\xi, \tag{55}$$

$$\hat{U}_2 = -\frac{1}{2\wp}\int_a^b e^{\xi\wp} g(\xi)\, d\xi, \tag{56}$$

and $g(\xi)$ represents the non-homogeneous term of the differential equation as

$$\begin{aligned} g(\xi) = \tfrac{c\,\cosh\xi}{e^{-k\xi/2}} \Big\langle & -kG\,(c_{13}^0/c_{11}^0) + (\beta_1^0/c_{11}^0)\, e^{-\int_0^t \psi(\tau)\, d\tau} \left\{ \tfrac{2}{\ell} e^{-k\xi/2} \right. \\ & \times \textstyle\sum_{n=0}^{\infty}\sum_{m=1}^{\infty} \left[e^{-\kappa\,\lambda_m^2 t} \left(\vartheta_0 G_0 + \tfrac{Q_i\,\kappa}{\lambda^0} \int_0^t e^{\kappa\,\lambda_m^2 \tau}\; \bar{\bar{\bar{f}}}(q_m, n,\, \tau)\, d\tau \right) \right] \\ & \times [k\, S_m + S_m'] \,\sin\left(\tfrac{n\pi z}{\ell}\right) /N_m \left.\right\} \Big\rangle, \end{aligned} \tag{57}$$

in which the prime ($'$) denotes differentiation with respect to the variable ξ.

With the form Equation (50) in Equation (26) of the radial displacement, the stresses (3) become

$$\begin{aligned} \sigma_{\xi\xi} = & \tfrac{\gamma\, e^{(2\wp+k)\xi/2}}{2c\,\cosh\xi} \{ [C_1 + \hat{U}_1]((2\wp - k)\hat{U}_1' + \Lambda_1) \\ & - e^{(-2\wp\xi)}[C_2 + \hat{U}_2]\; ((2\wp + k)\hat{U}_2' + \Lambda_2) \} \\ & + \gamma\, e^{k\xi}[(c_{13}^0/c_{11}^0)\, G - (\beta_1^0/c_{11}^0)\, T\,], \end{aligned} \tag{58}$$

$$\begin{aligned} \sigma_{\eta\eta} = & \tfrac{\gamma e^{(2\wp+k)\xi/2}}{2c\,\cosh\xi} \{ [C_1 + \hat{U}_1]((c_{12}^0/c_{11}^0)(2\wp - k)\hat{U}_1' + \Lambda_3) \\ & - e^{(-2\wp\xi)}[C_2 + \hat{U}_2]((c_{12}^0/c_{11}^0)(2\wp + k)\hat{U}_2' + \Lambda_4) \} \\ & + \gamma\, e^{k\xi}[(c_{13}^0/c_{11}^0)\, G - (\beta_1^0/c_{11}^0)\, T], \end{aligned} \tag{59}$$

$$\begin{aligned}\sigma_{zz} = &\tfrac{\gamma e^{(2\wp+k)\xi/2}}{2c\,\cosh\,\xi}\,\{\,[C_1+\hat{U}_1\,][(c_{13}^0/c_{11}^0)(2\wp-k)\,\hat{U}_1'+\Lambda_5]\\ &-e^{-2\wp\xi}(C_2\,+\hat{U}_2)\,((c_{13}^0/c_{11}^0)(2\wp+k)\hat{U}_2'\,+\Lambda_6)\}\\ &+\gamma\,e^{k\xi}[(c_{13}^0/c_{11}^0)G-(\beta_3^0/c_{11}^0)\,T,\end{aligned} \tag{60}$$

in which

$$\Lambda_1=2(c_{12}^0/c_{11}^0)-k+2\wp,\;\;\Lambda_2=-2(c_{12}^0/c_{11}^0)+k+2\wp,$$

$$\Lambda_3=(c_{12}^0/c_{11}^0)[2\wp-k]+2\;\;,\;\;\Lambda_4=(c_{12}^0/c_{11}^0)[2\wp+k]-2,$$

$$\Lambda_5=(c_{13}^0/c_{11}^0)(2-k+2\wp),\;\;\Lambda_6=(c_{13}^0/c_{11}^0)(-2+k+2\wp).$$

7. Further investigation

7.1. The homogeneous case

For $\gamma=1$ and $k=0$, one obtains all material constants of the Equation (15), that are independent of radial coordinates, then $c_{ij}=c_{ij}^0,\;\alpha_i=\alpha_i^0,\,\lambda_i=\lambda^0$ and $c_v=c_v^0$. Taking homogeneous material constants into consideration, the temperature distribution and displacement reduces to

$$\begin{aligned}T\;(\xi,\;z,\;t)\;=&\tfrac{2}{\ell}\sum_{n=0}^{\infty}\sum_{m=1}^{\infty}\left[e^{-\kappa\,\lambda_m^2 t}\left(\vartheta_0 G_0+\tfrac{Q_i\,\kappa}{\lambda^0}\int_0^t e^{\kappa\,\lambda_m^2\tau}\;\bar{\bar{f}}(q_m,n,\;\tau)\,d\tau\right)\right]\\ &\times\;S_m(k_1/2,k_2/2,\xi,-q_m)\;\sin\left(\tfrac{n\pi\,z}{\ell}\right)\;e^{-\int_0^t\psi\,(\tau)\;d\tau}/N_m,\end{aligned} \tag{61}$$

$$u_\xi(\xi)=C_1\,e^{\xi}+C_2\,e^{-\xi}+\hat{U}_1\,e^{\xi}+\hat{U}_2\,e^{-\xi}, \tag{62}$$

in which

$$\hat{U}_1=\;\;\frac{1}{4}\int_a^b e^{-\xi}g(\xi)\,d\xi,\hat{U}_2=\frac{1}{4}\int_a^b e^{\xi}g(\xi)\,d\xi, \tag{63}$$

and

$$\begin{aligned}g(\xi)=c\,\cosh\,\xi\,\Big\langle&(\beta_1^0/c_{11}^0)\,e^{-\int_0^t\psi\,(\tau)\;d\tau}\left\{\tfrac{2}{\ell}\;\sum_{n=0}^{\infty}\sum_{m=1}^{\infty}\left[e^{-\kappa\,\lambda_m^2 t}\right.\right.\\ &\left.\left.\times\left(\vartheta_0 G_0+\tfrac{Q_i\,\kappa}{\lambda^0}\int_0^t e^{\kappa\,\lambda_m^2\tau}\;\bar{\bar{f}}(q_m,n,\;\tau)\,d\tau\right)\right]\;S_m'\;\sin\left(\tfrac{n\pi\,z}{\ell}\right)/N_m\right\}\Big\rangle.\end{aligned} \tag{64}$$

The thermo-mechanical boundary conditions to evaluate integration constants C_1 and C_2 are $\sigma_{\xi\xi}=0$, $\sigma_{\xi\eta}=0$, $\sigma_{\xi z}=0$ at $\xi=a,\;b$, where the last two conditions get automatically satisfied. Then, by virtue of Equations (5) and (62), Equation (58) can be rewritten as

$$\begin{aligned}&C_1[c_{12}^0+(\hat{U}_1'(a)+1)\,c_{11}^0]+C_2e^{-2a}[c_{12}^0-(\hat{U}_2'(a)+1)\,c_{11}^0]\\ &+G\,c\,\cosh(a)\;e^{-a}\,c_{13}^0\;=\;c\,\cosh(a)\;e^{-a}\,\beta_1^0\,T(a),\end{aligned} \tag{65}$$

$$\begin{aligned}&C_1[c_{12}^0+(\hat{U}_1'(a\omega)+1)\,c_{11}^0]+C_2e^{-2a\omega}[c_{12}^0-(\hat{U}_2'(a\omega)+1)\,c_{11}^0]\\ &+G\,c\,\cosh(a\omega)\,e^{-a\omega}\,c_{13}^0\;=\;c\,\cosh(a\omega)\,e^{-a\omega}\,\beta_1^0\;T(a\omega),\end{aligned} \tag{66}$$

in which $\omega = b/a$ is the outer radius to inner radius ratio. In more specific manner, we will consider $\omega = 1.05$ for thin and $\omega = 1.50$ for the thick functionally graded hollow cylinder. Apart from the boundary conditions along the radial direction, we should also examine the conditions at $z = 0$ and $z = \ell$. The last two conditions $\sigma_{\eta z} = 0$, $\sigma_{\xi z} = 0$ at $z = 0,\ \ell$ automatically gets fulfilled and the first condition $2\pi \int_a^b \sigma_{zz}\, \xi\, d\xi = 0$ at $z = 0,\ \ell$ gives

$$\begin{aligned} &C_1 \int_a^{a\omega} \left[\tfrac{e^{\xi}}{c\cosh\xi}(\hat{U}_1'(\xi)+2)\right] \xi\, d\xi + C_2 \int_a^{a\omega} \left[\tfrac{e^{-\xi}}{c\cosh\xi}\hat{U}_2'(\xi)\right] \xi\, d\xi + G\int_a^{a\omega} \xi\, d\xi \\ &= \int_a^{a\omega} \left[\tfrac{\beta_3^0}{c_{13}^0} T(\xi) - \tfrac{e^{\xi}}{c\cosh\xi}\left[\hat{U}_1(\xi)(\hat{U}_1'(\xi)+2) - e^{-2\xi}\, \hat{U}_2(\xi)\, \hat{U}_2'(\xi)\right]\right] \xi\, d\xi. \end{aligned} \tag{67}$$

From Equations (65), (66) and (67), we have

$$C_1 = \frac{A_4(B_2D_3 + D_2B_3) - A_2(B_4D_3 - D_4B_3) + A_3(-B_4D_2 - D_4B_2)}{A_1(B_2D_3 + D_2B_3) - A_2(B_1D_3 - D_1B_3) + A_3(-B_1D_2 - D_1B_2)}, \tag{68}$$

$$C_2 = \frac{A_1\,(B_4D_3 - D_4B_3) - A_4\,(B_1D_3 - D_1B_3) + A_3\,(B_1D_4 - D_1B_4)}{A_1\,(B_2D_3 + D_2B_3) - A_2\,(B_1D_3 - D_1B_3) + A_3\,(-B_1D_2 - D_1B_2)}, \tag{69}$$

$$G = \frac{A_1\,(B_2D_4 + D_2B_4) - A_2(B_1D_4 - D_1B_4) + A_4(-B_1D_2 - D_1B_2)}{A_1\,(B_2D_3 + D_2B_3) - A_2\,(B_1D_3 - D_1B_3) + A_3\,(-B_1D_2 - D_1B_2)}, \tag{70}$$

in which

$$A_1 = c_{12}^0 + (\hat{U}_1'(a)+1)c_{11}^0,\ A_2 = e^{-2a}[c_{12}^0 - (\hat{U}_2'(a)+1)c_{11}^0],\ A_3 = c\cosh(a)e^{-a}c_{13}^0,$$

$$A_4 = c\cosh(a)\, e^{-a}\beta_1^0 T(a), B_1 = c_{12}^0 + (\hat{U}_1'(a\omega)+1)c_{11}^0,$$

$$B_2 = e^{-2a\omega}[c_{12}^0 - (\hat{U}_2'(a\omega)+1)c_{11}^0],\ B_3 = c\cosh(a\omega)e^{-a\omega}c_{13}^0,$$

$$B_4 = c\cosh(a\omega)e^{-a\omega}\beta_1^0 T(a\omega), D_1 = \int_a^{a\omega} \left[\frac{e^{\xi}}{c\cosh\xi}(\hat{U}_1'(\xi)+2)\right] \xi d\xi,$$

$$D_2 = \int_a^{a\omega} \left[\frac{e^{-\xi}}{c\cosh\xi}\hat{U}_2'(\xi)\right] \xi d\xi, D_3 = \int_a^{a\omega} \xi d\xi,$$

$$D_4 = \int_a^{a\omega} \left\{ \left(\frac{\beta_3^0}{c_{13}^0}\right) T(\xi) - \frac{e^{\xi}}{c\cosh\xi}\left[\hat{U}_1(\xi)(\hat{U}_1'(\xi)+2) - e^{-2\xi}\hat{U}_2(\xi)\hat{U}_2'(\xi)\right] \right\} \xi d\xi.$$

It can be concluded that the stress component vanishes everywhere in a homogeneous transversely isotropic hollow cylinder when it is impacted by uniformly heated heat supply with $\gamma = 0$ and $k > 0$ as the inhomogeneity parameter. It is also observed that as $k \to 0$, then, $c_{ij} = c_{ij}^0\, \gamma$ and $\alpha_i = \alpha_i^0\, \gamma \to$ constant, irrespective of γ. One discovers that all material constants are independent of the radial coordinate and governing equation reduces to the Euler differential equation.

7.2. The inhomogeneous case

For the inhomogeneity parameter $\gamma \neq 1$ and $k \neq 0$, the radial stress expression (58) can be rewritten utilising thermo-mechanical boundary conditions (7) as

$$\begin{aligned}&C_1[(2\wp - k)\hat{U}_1' + \Lambda_1] - C_2\, e^{(-2\wp a)}[(2\wp + k)\hat{U}_2' + \Lambda_2] + 2\,c\,\cosh a\\ &\times e^{(k-2\wp)\,a/2}(c_{13}^0/c_{11}^0)\,G = \;2c\,\cosh a\, e^{(k-2\wp)\,a/2}(\beta_1^0/c_{11}^0)\,T\\ &-\hat{U}_1((2\wp - k)\hat{U}_1' + \Lambda_1) + \hat{U}_2 e^{(-2\wp a)}\,((2\wp + k)\hat{U}_2' + \Lambda_2),\end{aligned} \tag{71}$$

$$\begin{aligned}&C_1((2\wp - k)\hat{U}_1' + \Lambda_1) - C_2\, e^{(-2\wp\, a\,\omega)}((2\wp + k)\hat{U}_2' + \Lambda_2) + 2c\,\cosh\; a\\ &\times e^{(k-2\wp)\;a\omega/2}(c_{13}^0/c_{11}^0)\,G \;=\; 2c\,\cosh\; a\, e^{(k-2\wp)\;a\,\omega/2}(\beta_1^0/c_{11}^0)\,T\\ &-\hat{U}_1((2\wp - k)\hat{U}_1' + \Lambda_1) + \hat{U}_2 e^{(-2\wp\; a\,\omega)}\,((2\wp + k)\hat{U}_2' + \Lambda_2).\end{aligned} \tag{72}$$

As pointed out by [Spencer et al. (1992)], the form of solution considered, does not permit the point-by-point specification of traction at the two ends $z = 0$ and $z = \ell$. Only resultant forces and moments can be specified on the basis of Saint Venant's principle. From the problem we have considered, we get the boundary condition (6) as

$$\begin{aligned}&C_1 \int_a^{a\omega} \left[c_{13}^0(-k + 2\wp)\hat{U}_1'(\xi) + \Lambda_5\right]\xi d\xi - C_2 \int_a^{a\omega} e^{-2\wp\xi}\left[c_{13}^0(k + 2\wp)\hat{U}_2'(\xi) + \Lambda_6\right]\xi d\xi\\ &-2\,G\,c\int_a^{a\omega}\left[\cosh\xi e^{(3k+2\wp)\xi/2}c_{13}^0\right]\xi d\xi = \int_a^{a\omega}\left[\cosh\xi e^{(3k+2\wp)\xi/2}\beta_1^0 T\right]\xi d\xi\\ &+\int_a^{a\omega}\left\{\hat{U}_2(\xi)e^{-2\wp\xi}\left[c_{13}^0(k + 2\wp)\hat{U}_2'(\xi) + \Lambda_6\right] - \hat{U}_1(\xi)\left[c_{13}^0(-k + 2\wp)\hat{U}_1'(\xi) + \Lambda_5\right]\right\}\xi d\xi.\end{aligned} \tag{73}$$

The general expressions for stress and displacement contain unknown integration constants C_1, C_2 and unknown coefficient constant G. For the determination of all three unknown constants, there are three non-redundant conditions (71), (72) and (73) available. It is also observed that displacement function u is continuous at $\xi = a$ and b, and $\sigma_{\xi\xi}$ vanishes at the inner and outer boundary of the circular hollow cylinder.

8. Numerical Results, Discussion and Remarks

For mathematical computations, we have considered two materials as (i) hexagonal Zinc as Material I [Sharma and Sharma (2002)] which is nearly isotropic, (ii) Lithium Tantalate as Material II [www.korth.de (1999)] which is an anisotropy in nature, in a particular case. Data of the physical properties are enlisted in Table 1 and Table 2 and shown below For the sake of simplicity of calculation, we introduce the following dimensionless values

$$\bar{\xi} = \xi/b, \bar{z} = z/b, \bar{T} = T/T_0, \tau = \kappa t/b^2, \bar{u}_\xi = u_\xi/(c_{11}^0\alpha_1^0 T_0), \bar{\sigma}_{\xi\xi} = \sigma_{\xi\xi}/(c_{11}^0\alpha_1^0 T_0),$$

$$\bar{\sigma}_{\eta\eta} = \sigma_{\eta\eta}/(c_{11}^0\alpha_1^0 T_0), \bar{\sigma}_{zz} = \sigma_{zz}/(c_{11}^0\alpha_1^0 T_0).$$

The physical parameters as $a = 0.95$ m (thin), $a = 0.67$ m (thick), $b = 1$ m, $\ell = 0.08$m, $k_1 = k_2 = 0.86$ (assumed value) and reference temperature as $T_0 = 423\,K$. The q_m =1.531, 1.648, 2.745, 6.086, 7.001, 8.1178, 9.543, 10.631, 12.112, 14.123, 17.238, 19.734,… are the positive and real roots of the $Ce_m(\alpha_1, a,\, q_m)Fey_m(\alpha_2, b,\, q_m) - Ce_m(\alpha_2, b,\, q_m)Fey_m(\alpha_1, a,\, q_m) = 0$. Figures

Table 1. Thermo-mechanical material properties

Parameters	Material I	Material II
Elastic constants [10^{11} N/m^2]		
c_{11}^0	1.628	2.300
c_{12}^0	0.362	0.420
c_{13}^0	0.508	0.790
c_{33}^0	0.627	2.760
Thermal conductivity [W/mK] λ^0	1.384	4.600
Thermal expansion coefficient [10^{-6} /K]		
α_1^0	1. 798	4.00
α_3^0	1.383	16.00
Heat capacity coefficient [10^2 J/kgK] c_v^0	3.90	4.24
Mass density [10^3 kg/m^3] ρ^0	7.140	7.454

Table 2. Material properties in dimensionless form

Details	c_{12}^0/c_{11}^0	c_{13}^0/c_{11}^0	c_{33}^0/c_{11}^0	α_3^0/α_1^0
Material I	0.222	0.312	0.385	0.769
Material II	0.183	0.343	1.200	4.000

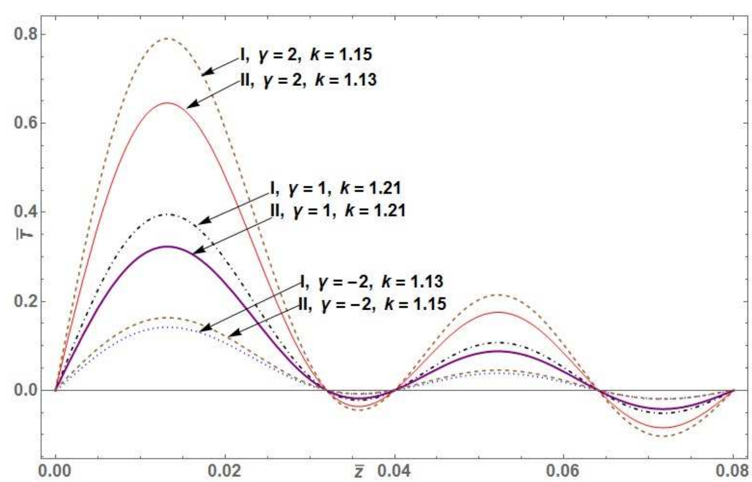

Figure 2. Temperature distribution along $\bar{z}$- direction.

2- 4 are typical dimensionless plots of temperature distribution. Figure 2 shows temperature distribution along $\bar{z}$- direction for different values of $\bar{\xi}$ and the fixed value of time parameter τ , in which graphs are sinusoidal in nature and attains zero temperature at both inner and outer edges a and b. In Figure 3 temperature distribution along $\bar{\xi}$ for different values of $\bar{z}$ and fixed time τ , whereas in Figure 4 temperature distribution along time parameter τ for different values of $\bar{\xi}$ and fixed value of $\bar{z}$, are gradually increases at the outer edge. Figures 5- 9 illustrates the radial, tangential and axial stress distribution along the radius for different time parameter and fixed $\bar{z}$ in a thin functionally graded hollow cylinder. When the inhomogeneity parameters are considered as $\gamma \neq 0$ and $k \neq 0$,

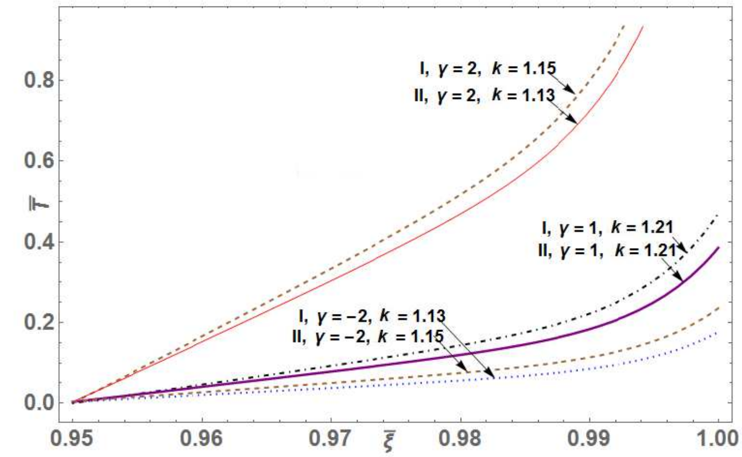

Figure 3. Temperature distribution along $\bar{\xi}$-direction.

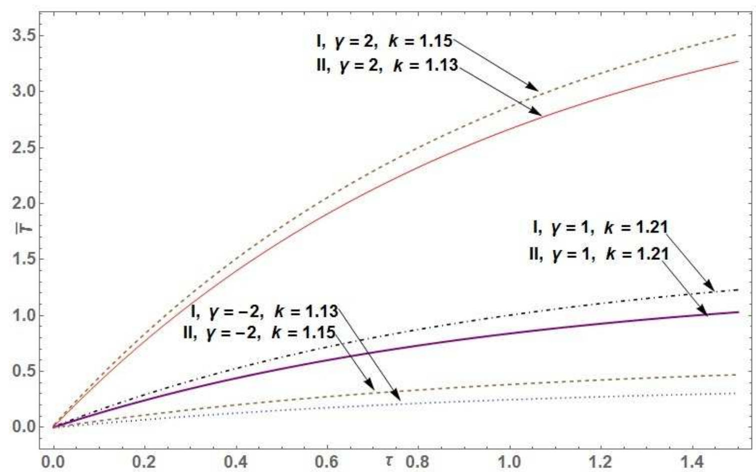

Figure 4. Temperature distribution along time τ.

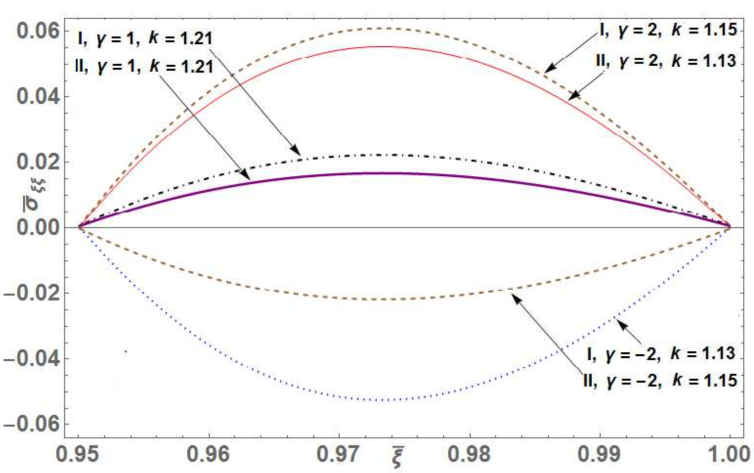

Figure 5. Radial stress $\bar{\sigma}_{\xi\xi}$ along $\bar{\xi}$- direction.

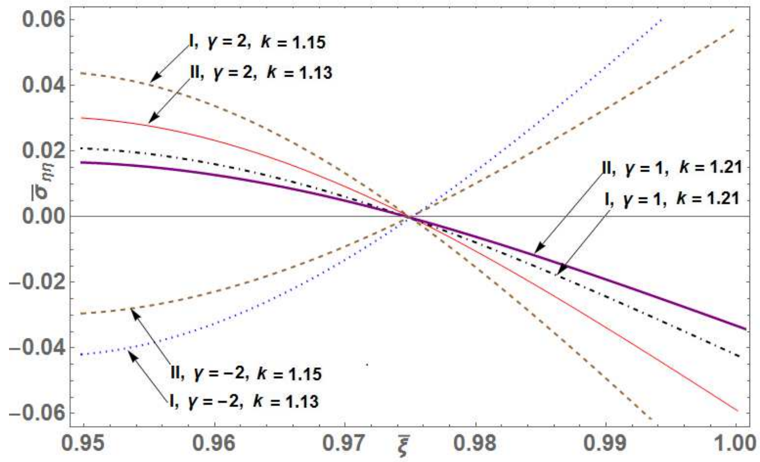

Figure 6. Tangential stress $\bar{\sigma}_{\eta\eta}$ along $\bar{\xi}$ - direction.

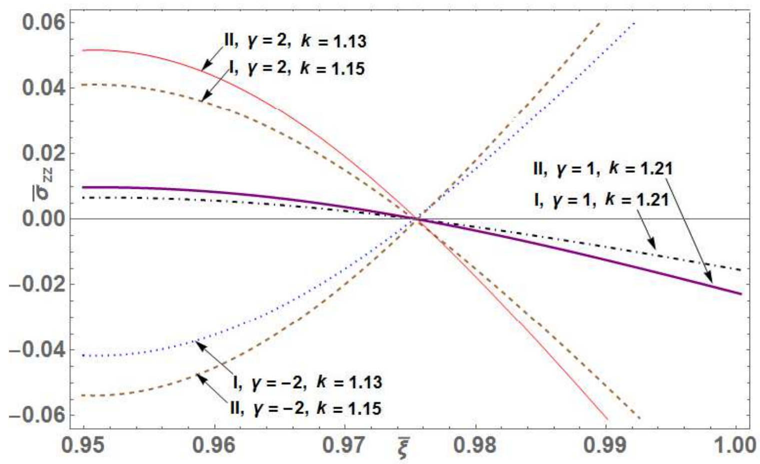

Figure 7. Axial stress $\bar{\sigma}_{zz}$ along $\bar{\xi}$- direction.

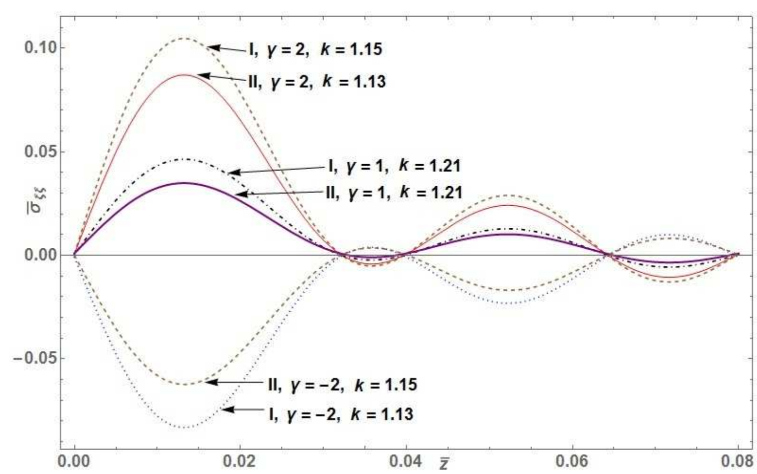

Figure 8. Radial stress $\bar{\sigma}_{\xi\xi}$ along $\bar{z}$- direction.

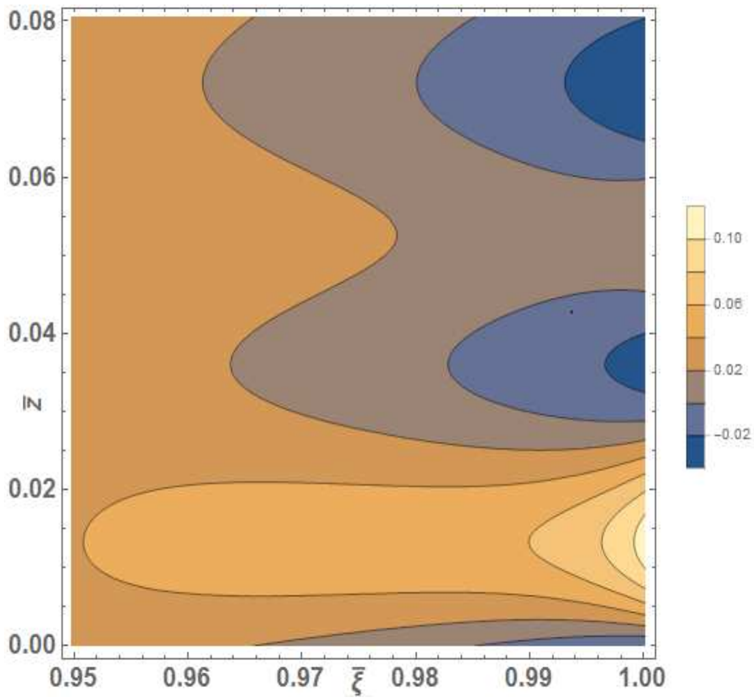

Figure 9. Tangential and Axial stresses along $\bar{z}$- direction.

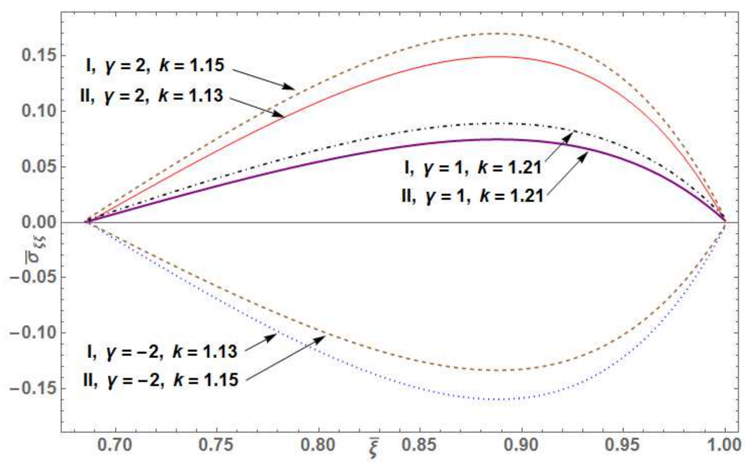

Figure 10. Radial stress $\bar{\sigma}_{\xi\xi}$ along $\bar{\xi}$- direction for $\omega = 1.5$.

the non-dimensional radial stress response are maximum at the interior, and so the outer edges of the cylinder tend to expand more than the inner core, leading to the inner part being under tensile stress. In particular, for negative γ the radial stress also decreases at fixed radius leading to compressive radial stress. Also for negative γ, both the tangential and axial stress components change from negative at the inner surface to positive at the outer surface and vice-versa. The distribution $\bar{\sigma}_{\eta\eta}$ and $\bar{\sigma}_{zz}$ in the thin hollow cylinder are nearly parabolic along the radial direction. Figures 8, it is seen that the radial stress along $\bar{z}$- direction for different values of $\bar{\xi}$ and the fixed value of time τ follows a sinusoidal characteristic with both extreme at zero. Similar trends were also noticed for the tangential and axial stresses along $\bar{z}$- direction for different values of $\bar{\xi}$ and the fixed value of time τ as shown in contour Figure 9. Figures 10- 12 illustrates the radial, tangential and axial stress

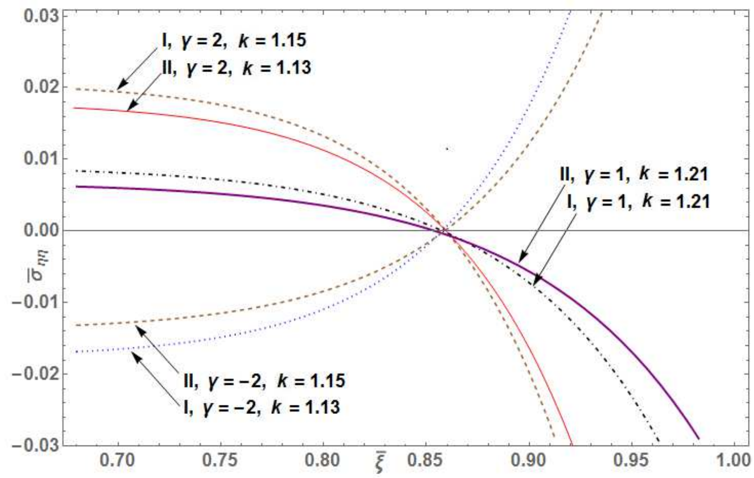

Figure 11. Tangential stress $\bar{\sigma}_{\eta\eta}$ along $\bar{\xi}$ - direction for $\omega = 1.5$.

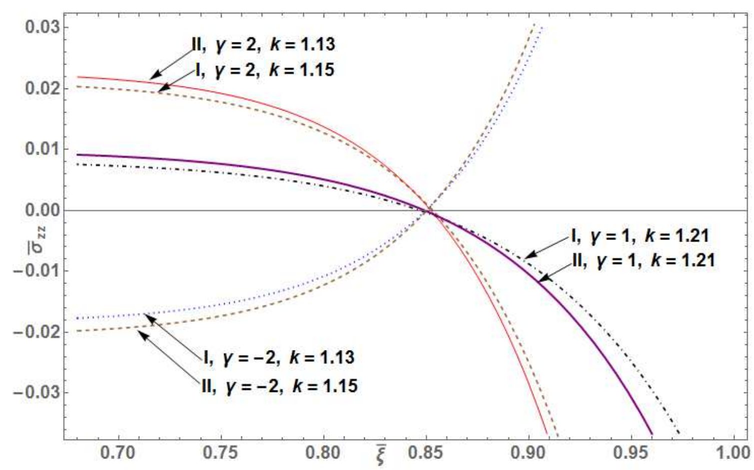

Figure 12. Axial stress $\bar{\sigma}_{zz}$ along $\bar{\xi}$- direction for$\omega = 1.5$.

distribution along the radius for a thick functionally graded hollow cylinder, given for comparison. It is observed from all figures that the outcome agrees with the earlier declared results [Chen et al. (2002)].

9. Conclusion

An analytical solution is achieved for the two-dimensional axisymmetric thermoelastic problem of a transversely isotropic functionally graded hollow cylinder is subjected to a transient temperature field, and the material properties are of parabolic power-law functions of the radial coordinates. The solution and graph trends are verified by comparing with the solution of the uniformly heated hollow cylindrical shell [Chen et al. (2001)] as well as cylinder [Chen et al. (2002)] available in the literature.

It is found that the reduction in the thickness reduces the magnitudes of stresses and deformation. It is observed from the numerical results that γ have a significant effect on thermoelastic stresses. Hence it is possible to make more efficient use of the material with an appropriate choice of gradient parameters γ and k in engineering applications to design a hollow cylinder. It is also observed that for a transversely isotropic homogeneous hollow cylinder, stress response are negligible compared with the functionally graded material. The method of the solution presented in this paper is useful in the analysis of functionally graded hollow cylinder with transverse isotropy for optimising the design in terms of material usage and performance.

The above solution can easily degenerate into isotropic functionally graded hollow cylinder for the thermoelastic problem. On setting the physical parameters [Chen et al. (2001)] as $c_{11} = c_{33} = \lambda + 2\mu$, $c_{44} = \mu$, $c_{12} = c_{13} = \lambda$, $\lambda = E\upsilon/[(1+\upsilon)(1-2\upsilon)]$ and $\mu = E/[2(1+\upsilon)]$ respectively, where E is Young's modulus, υ is Poisson's ratio, and λ and μ are Lame elastic (Lame's) constant.

Acknowledgment:

The authors are grateful to Prof. N.K. Choubey and Prof. A.M. Haghighi for their valuable suggestion and constructive comments which resulted in revising the paper to its present form.

REFERENCES

Abrinia, K. Naee, H., Sadeghi, F. and Djavanroodi, F. (2008). New analysis for the FGM thick cylinders under combined pressure and temperature loading, American Journal of Applied Sciences, Vol. 5, No. 7, pp. 852-859.

Asemi, K., Ashrafi, H. and Salehi, M. (2013). Three-dimensional static and dynamic analysis of functionally graded elliptical plates, employing graded finite elements, Acta Mechanica, Vol. 224, No. 8, pp. 1849-1864.

Bhad, P., Varghese, V. and Khalsa, L. (2016). Transient thermoelastic problem in a confocal elliptical disc with internal heat sources, Advances in Mathematical Sciences and Applications, Tokyo, Japan, Vol. 25, No. 1, pp. 43-61.

Bhad, P., Varghese, V. and Khalsa, L. (2017). Heat source problem of thermoelasticity in an elliptic plate with thermal bending moments, Journal of Thermal Stresses, Vol. 40, No. 1, pp.96-107.

Bhad, P., Varghese, V. and Khalsa, L. (2017). Thermoelastic-induced vibrations on an elliptical disk with internal heat sources, Journal of Thermal Stresses, vol. 40, No. 4, pp. 502-516.

Bhad, P., Varghese, V. and Khalsa, L. (2017). A modified approach for the thermoelastic large deflection in the elliptical plate, Archive of Applied Mechanics, Vol. 87, No. 4, pp. 767-781.

Chen, W., Ye, G., and Cai, J. (2001). A uniformly heated functionally graded cylindrical shell with transverse isotropy, Mechanics Research Communication, Vol. 283, No. 5, pp. 535-542.

Chen, W., Ye, G., and Cai, J. (2002). Thermoelastic Stresses in a uniformly heated functionally graded isotropic hollow cylinder, J. of Zhejiang University SCIENCE, Vol. 3, No. 1, pp. 1-5.

Cheng, Z.-Q., and Batra, R.C. (2000). Three-dimensional thermoelastic deformations of a functionally graded elliptic plate, Composites: Part B, Vol. 31, pp. 97-106.

El Dhaba, A.R., Ghaleb, A.F. and Abou-Dina, M.S. (2003). A problem of plane, uncoupled linear thermoelasticity for an infinite, elliptical cylinder by a boundary integral method, Journal of Thermal Stresses, Vol. 26, No. 2, pp. 93-121.

Eraslan, A.N. and Akis, T. (2005). Elastoplastic response of a long functionally graded tube subjected to internal pressure, Turkish J. Eng. Env. Sci., Vol. 29, pp. 361-368.

Hasheminejad, S.M., Rezaei, S. and Hosseini, P. (2011). Exact solution for dynamic response of an elastic elliptical membrane, Thin-Walled Structures, Vol. 49, pp. 371-378.

Horgan C.O. and Chan A.M. (1999). The pressurised hollow cylinder or disk problem for functionally graded isotropic linearly elastic material, Journal of Elasticity, Vol. 55, pp. 43-59.

Hsieh, J.-J., and Lee, L.-T. (2006) An inverse problem for a functionally graded elliptical plate with large deflection and slightly disturbed boundary, International Journal of Solids and Structures, Vol. 43, No. 20, pp. 5981-5993.

Kamdi, D.B., Khobragade, N.W. and Varghese, V. (2008). Thermoelastic problem of a uniformly heated functionally graded rotating solid shaft, International Journal of Applied Mathematics, vol. 21, No. 2, pp. 215-226.

Khorshidvand, A.R., Khalili, S.M.R. and Branch, S.T. (2010). A new analytical solution for deformation and stresses in functionally graded rotating cylinder subjected to thermal and mechanical loads, International Conference on Continuum Mechanics (5TH IASME-WSEAS), Cambridge, UK, pp. 201-204, February 23-25.

Khorshidvand, A.R. and Jabbari, M. (2012). Deformation and stresses analysis in FG rotating hollow disk and cylinder subjected to a thermal and mechanical load, Applied Mechanics and Materials, Vol. 187, pp. 68-73.

Khorshidvand, A.R. and Jabbari, M. (2012). Thermomechanical analysis in FG rotating hollow disk, Applied Mechanics and Materials, Vol. 110, pp. 148-154.

Kumar, B.R., Ganesanand, N., Sethuraman, R. (2009). Vibro-Acoustic analysis of functionally graded elliptic disc under thermal environment, Mechanics of Advanced Materials and Structures, Vol. 16, No. 2, pp. 160-172.

Lutz M.P. and Zimmerman R.W. (1999). Thermal stresses and thermal expansion in a uniformly heated functionally graded cylinder, J. of Thermal Stresses, Vol. 22, pp. 177-188.

McLachlan, N.W. (1947). *Theory and Application of Mathieu function, Clarendon Press*, Oxford.

Obata Y. and Noda N. (1994). Steady thermal stresses in a hollow circular cylinder and a hollow sphere of a functionally gradient material, Journal of Thermal Stresses, Vol. 17, pp. 471-478.

Sharma J.N. and Sharma P.K. (2002). Free vibration analysis of homogeneous transversely isotropic thermoelastic cylindrical panel, J. of Thermal Stresses, Vol. 25, No. 2, pp. 169-182.

Sneddon, I.N. (1995). *Fourier transforms*, McGraw-Hill, New York, pp. 194.

Spencer, A.J.M., Watson, P. and Rogers, T.G. (1992). Thermoelastic distortions in laminated anisotropic tubes and channel section, Journal of Thermal Stresses, Vol. 15, pp. 129-141.

Varghese, V. and Khobragade, N.W. (2008). Thermoelastic behaviour of a uniformly heated functionally graded cylindrical shell with parabolic-varying properties, Advances in Mathematical Sciences and Application, vol. 18, No. 1, pp. 595-605.

Varghese, V. and Khobragade, N.W. (2008). Mathematical analysis of functionally graded hybrid composite channel section in the interfacial zone during post-solidification cooling, Advances and Applications in Fluid Mechanics, Vol. 3, No. 1, pp. 41-55.

Wang, T.J., Fan, L.F. and Shao, Z.S. (2004). Analytical solutions of stresses in functionally graded circular hollow cylinder with finite length,Key Eng. Materials, Vol. 261-263, pp. 651-656.
http://www.korth.de/index.php/162/items/20.html